

The Discovery of an Aromatic Silicon Aluminium Compound Through A Novel Four-Pronged Computational Approach

Himanshu Sharma,^[a,b] and Kumar Vanka^{*[a,b]}

^aPhysical and Materials Chemistry Division, CSIR-National Chemical Laboratory, Dr. Homi Bhabha Road, Pashan, Pune 411008, India

^bAcademy of Scientific and Innovative Research (AcSIR), Ghaziabad 201002, India

*Corresponding: k.vanka@ncl.res.in

KEYWORDS: Main Group Molecule, 2π aromaticity, AINR, Four-membered aromatic ring, First-principles

ABSTRACT

Traditional experimental methods for the design of molecules are time-consuming and inefficient, prompting a shift towards computational approaches. Here, we unveil a strategy that transcends traditional paradigms. Rooted in first principles and liberated from experimental constraints, our newly developed four-stage approach allows the discovery of new molecules that display interesting properties. The current work showcases an interesting molecule that has been discovered through this approach: a four membered cyclic compound of silicon and aluminium that displays 2π aromaticity, and capable of the activation of important small molecules.

Designing new molecules, whether through computation or experimentation, poses a significant challenge in chemistry, aiming for reactivity, selectivity, and stability. Traditional reaction-based screening in experiments is inefficient and time-consuming, leading scientists to turn to computational models for enhanced efficiency.¹

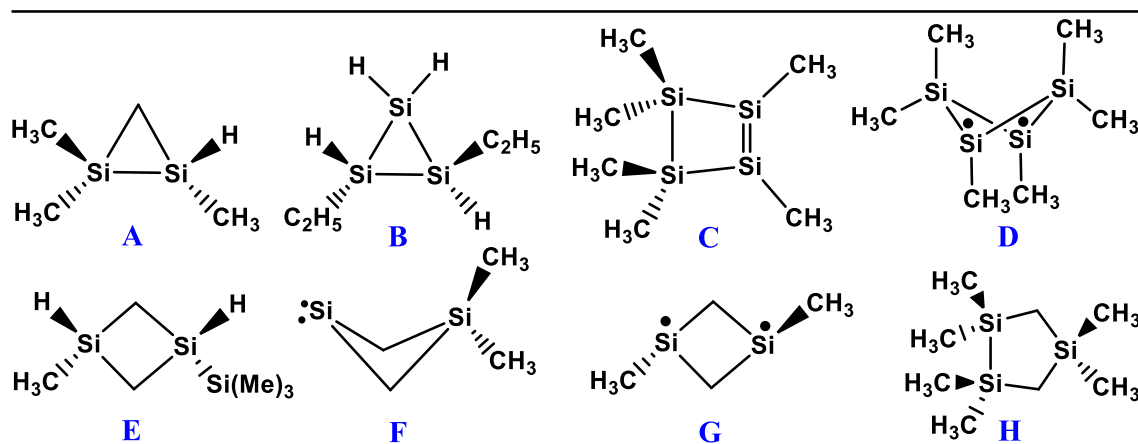
Computational chemistry, powered by quantum calculations, is vital in grasping reaction mechanisms and actively shaping molecule design. It entails two facets: one emphasizes physical properties, integrating data science and machine learning with translation challenges,² still in early development; the other delves into atomic-level reaction mechanisms.^{3,4} While providing detailed insights, precision requirements constrain the explored chemical space. Computational traditional methods involve creating libraries of potential molecules, escalating time and cost with library growth. Recently, inverse design methods have emerged, optimizing chemical structures from desired properties using techniques like gradient-based optimization, alchemical transformations, and machine learning.⁵ Though these methods' application to catalysis is in early stages, ongoing development promises robust computational catalyst design.

The intricate nature of molecule design, marked by multiscale considerations, intricate multistep mechanisms, and dependencies on experimental conditions, introduces formidable challenges. Given this complexity, no singular computational strategy universally prevails for molecule design.

Here, we present an innovative molecular design strategy grounded in first principles, independent of experimental input. The approach involves four key stages: (1) molecular skeleton formulation - using the AINR (*ab-initio* nanoreactor) method,⁶ a logical algorithm predicts reasonable molecular structures efficiently without relying on experimental data. AINR, based on AIMD, introduces a virtual piston to enhance collision dynamics and surmounting barrier, allowing exploration of reaction pathways computationally, (2) stability validation: rigorous DFT calculations^{7,8} ensure stability on the potential energy surface (PES) of the generated molecular skeleton, enhancing confidence in the proposed structure, (3) optimal molecule refinement: iteratively refining the optimal molecule involves adjusting ligands guided by energy and magnetic based criteria such as aromaticity,⁹ AIM analysis,¹⁰ and conceptual DFT,¹¹ ensuring the identification of promising candidates, and (4) practical applications identification: the potential applications of the optimized molecule are systematically identified based on its structure, reactivity, and stability. This comprehensive approach aims to contribute valuable insights to molecular design.

In this work, we are pioneering this strategy to discover new Si-containing aromatic molecules. Aromaticity, vital in understanding benzene's stability,¹² extends to organometallic and inorganic realms with theories like Mobius,¹³ Spherical,¹⁴ 3D,¹⁵ Baird,¹⁶ Fowler,¹⁷ metalla,¹⁸ dismutational,¹⁹ and multifold aromaticities.²⁰ In the pursuit of Si-containing aromatic molecules, we initially employed a Si-based reaction mixture with 10 dimethylsilylene molecules in AINR⁶ to validate our method (more details refer to ESI). The impracticality of incorporating bulky groups on the Si center arises from AINR's collision nature, leading to molecule fragmentation. Our simulation, focused on generating molecular skeletons, resulted in diverse cyclic products showcased in Scheme 1. Notably, during the simulation, numerous products were formed and simultaneously destroyed due to AINR's collision and relaxation processes. Consequently, our analysis selectively prioritizes molecules with prolonged lifespans, enhancing our understanding of structural stability

and reactivity. Analysis of the nanoreactor products (scheme 1) underscores the successful synthesis and practical application of these molecules through judicious Si ligand selection.



Scheme 1. The results of the AINR method has been shown here.

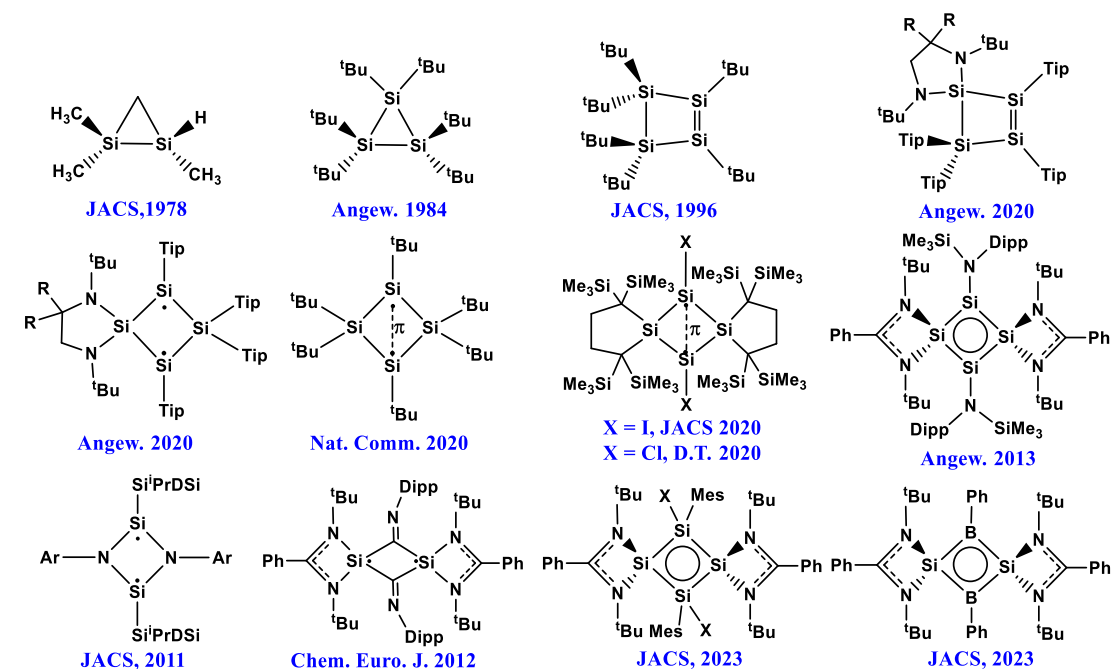
Pedde *et al.* showcased the tetramethyldisilene rearrangement,²¹ yielding disilacyclopropane—the product **A** observed in our AINR results. For a concise comparison between nanoreactor products and reported molecules, all synthesized compounds are outlined in Scheme 2. Schnering *et al.* synthesized hexa-tert-butylcyclotrisilane, a colorless, air, and heat-stable cyclo-trisilane (molecule **B**).²²

In the exploration for homogeneous four-membered rings (4-MRs), our inquiry yielded the planar hexakis-cyclodisilene molecule **C**, a milestone marked by Kabuto *et al.* as the first stable cyclodisilene.²³ Employing ^tBu as an apt ligand for the Si center, they successfully synthesized hexakis(tert-butyl dimethylsilyl)tetrasilacyclobutene. Alongside, we obtained a diradicaloid, represented by molecule **D** in Scheme 1. The optimized puckered structure of **D** exhibits a Si-Si bond length between radical Si atoms at 2.89 Å notably surpassing the previously reported longest Si-Si bond (^tBu₃Si-Si ^tBu₃, 2.697 Å).²⁴ The DFT calculations for molecules **C** and **D** suggest comparable energies on the potential energy surface ($\Delta G = 0.1$ kcal/mol). However, the trans isomer of molecule **D**, while featuring planarity at the Si₄ ring, is energetically elevated by 12.7 kcal/mol compared to **D**.

In 2020, D. Scheschkewitz achieved a groundbreaking milestone by synthesizing the first homonuclear diradicaloid with a Si₄ planar ring,²⁵ featuring one unpaired electron on both Si atoms

at 1,3 position. Prior to this accomplishment, Iwamoto *et al.* had reported an isolable tetrasilicon analogue of a planar bicyclo[1.1.0]butane, where bridgehead Si atoms formed a π bond.²⁶ Subsequent literature extensively documented the existence of planar homonuclear Si₄ rings, with 1,3 Si atoms exhibiting a single π bond.²⁷ This body of work collectively substantiates and validates the formation of molecule **D** through the AINR method, further advancing our understanding of novel silicon-based structures.

In the exploration of heteronuclear 4-membered rings (4-MRs), we identified molecule **E**, featuring a Si₂C₂ ring in a planar configuration as proposed by Pannell *et al.*²⁸ Additionally, we obtained silylene-type puckered molecule **F** and shortly observed the planar diradicaloid molecule **G**. The DFT calculations revealed that **G** is energetically less favorable, being 19.3 kcal/mol higher than **F**. In 2011, A. Sekiguchi's team achieved a breakthrough, synthesizing the first Si analogue isolable heteronuclear planar diradicaloid with a Si₂N₂ 4-MR.²⁹ This pivotal advancement underscores the critical role of ligand selection in shaping the formation of molecule **G**. The diverse range of products obtained *via* the AINR method, each demonstrating practical feasibility with appropriate ligands, firmly attests to the reliability of the method and its efficacy in uncovering novel molecular structures.

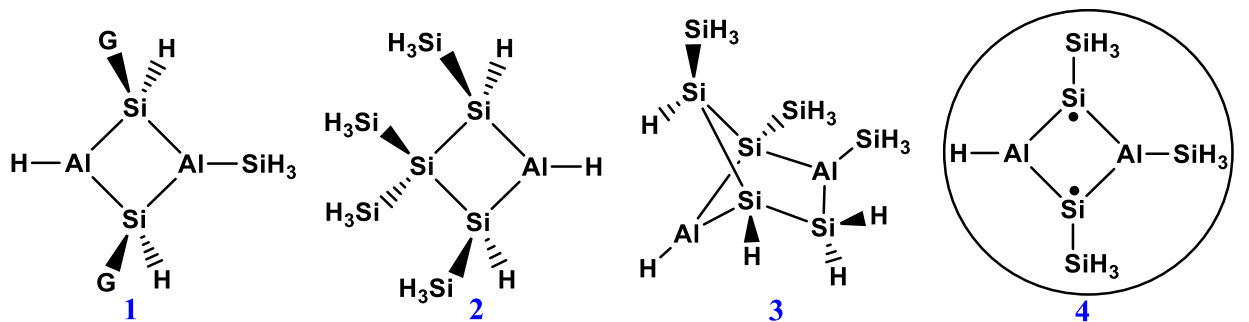


Scheme 2. All experimentally synthesized molecules, whose skeletal structures have been obtained through the AINR method, are depicted here.

The molecules obtained from the discussed AINR approach, alongside its 4-MRs products and synthetic counterparts, exemplifies the synthesis of stable biradical molecules through selective ligand choices. Central to this process is the presence of two unpaired electrons at the 1,3 positions within the Pz orbitals, prompting a pertinent question: can strategic atom placement at the 2,4 positions of 4-MRs facilitate effective interaction with these electrons, enabling the delocalization of these 2π electrons across the 4-MRs? Neutral inorganic molecules rarely exhibit 2π aromaticity; charged counterparts, while showcasing it, suffer from diminished stability due to factors like charge repulsion and structural reactions.^{30,31,32} Homogeneous Si_4 rings seldom display 2π aromaticity. In 2023, Zhu and Cui reported the first neutral 2π aromatic planar rhombic Si_4 ring,³³ emphasizing dominant π aromaticity in a saturated ring. Conversely, a 2013 study by So *et al.* highlighted a neutral $4\pi e$ homogeneous Si_4 ring, demonstrating unique dismutational aromaticity, not conventional π aromaticity.³⁴ Literature indicates that introducing heteroatoms at alternate positions in Si_4 rings promises to unlock the coveted realm of 2π aromaticity.³⁵ This structural refinement, poised to elevate system stability, not only captivates the scientific imagination but also beckons us towards an alluring frontier of unprecedented exploration and discovery.

In our quest for Si-based heteronuclear 4-MRs, we utilized a mixture of 10 SiH_2 and 10 AlH_3 molecules as the primary Si and Al source. The simulation yielded various cyclic products, some of which are depicted in Scheme 3. Notably, molecule **1** exhibited prolonged presence throughout the simulation, followed by molecules **2** and **3**, albeit to a lesser extent. Additionally, we identified a heteronuclear Si_2Al_2 -containing ring (molecule **4**, Scheme 3). This structure, characterized by mono-substituted ring vertices, exhibited a recurring presence despite its brief lifespan during the simulation. This phenomenon, indicative of its resilience, offers profound insights, elevating the ring to a compelling subject for further exploration and detailed study. The optimized parent structure, $\text{Si}_2\text{Al}_2\text{H}_4$, exhibits a planar rhombic geometry with Si atoms separated by 2.9 Å—remarkably surpassing the reported longest Si-Si bond (${}^t\text{Bu}_3\text{Si-Si}^t\text{Bu}_3$, 2.697 Å).²⁴ Each Si-Al bond

length is 2.36 Å, shorter than the typical Si-Al single bond (2.45 Å)³⁶³⁷³⁸³⁹ suggesting electron delocalization. Moreover, a substantial HOMO-LUMO gap of 3.9 eV and the widespread HOMO localization across the Si₂Al₂ ring, enhance the intrigue, motivating further investigations with diverse ligands.



Scheme 3. The results of the AINR method have been shown here.

Aligned with the existing literature and our preceding discussions, ligands play a crucial role in stabilizing the biradicaloid and establishing a planar ring structure. We categorize ligand selection into two distinct types, namely for the Si center and the Al center. For the Si center, we opted for two types of ligands—Phosphino and amidinated—whose optimized structures are depicted in Figure 1. As per the literature, the stabilization of 4-MRs is suggested through the use of bulky or chelating group ligands.³⁴⁴⁰⁴¹⁴² The DFT geometry analysis reveals that the phosphino ligand results in a puckered Si₂Al₂ ring with Si-Al bond lengths ranging from 2.38 to 2.41 Å and a dihedral angle of 39.06°. Conversely, the amidinated ligand induces a Si₂Al₂ ring with a dihedral angle of 4.68°, uniform bond lengths of 2.37 Å between all Si-Al bonds, a Si-Si distance of 3.32 Å, and an Al-Al distance of 3.37 Å, suggesting a fully square planar ring. This remarkable structural configuration, characterized by complete planarity, uniform bond equalization shorter than actual Si-Al single bonds, and the presence of two free electrons within the ring, captivates our attention by invoking the Hückel aromaticity rule.⁴³ This principle asserts that cyclic, planar molecules containing (4n+2) π electrons exhibit aromaticity, underscoring the remarkable aromatic character inherent within this novel molecular framework. In a recent advancement in 2023, Roesky⁴⁴ and Su⁴⁵ independently reported have unveiled boron analogues of these neutral, planar 4-MR,

revealing compelling 2π aromaticity within the ring structure. This significant revelation further serves to underscore the efficacy and robustness of our strategic approach in molecular design.

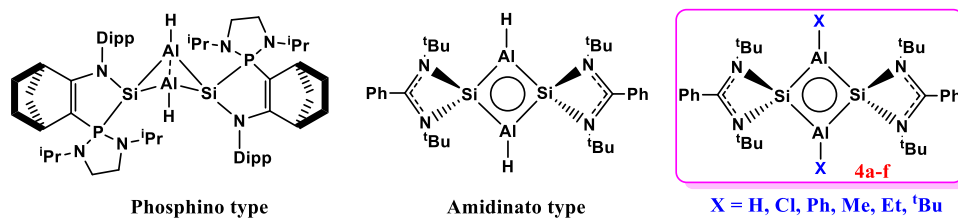


Figure 1. The optimised geometries of both type ligands have been shown here. The DFT calculations have been performed at B3LYP-D3/def2TZVP level of theory.

Moreover, to delve deeper into the structural exploration of this groundbreaking molecule, we introduced six distinct ligands (H, Cl, Ph, Me, Et, and ^tBu) on the Al center, while maintaining the amidinated ligand on Si atoms. The resulting molecules are denoted as **4a** to **4f**, as illustrated in Figure 1. The optimized geometry of molecules **4a** to **4f** indicates uniform Si-Al bond lengths, ranging from a minimum of 2.35 Å for **4b** to a maximum of 2.37 Å for **4c** and **4f**, with **4a**, **4d**, and **4e** exhibiting 2.36 Å. The highest dihedral angle is observed for **4b** (X=Cl) at 11.45°, while the lowest is found for **4c** (X=Ph) at 3.9°. (Please refer to Table S1) Similarly, the HOMO-LUMO analysis across all molecules reveals an energy gap within the range of 2.44-2.74 eV (see Table S2 & Figures S1-S7) where HOMO is completely localised over Si₂Al₂ ring.

To comprehend the molecular structure, bonding, and magnetic behaviour of our novel molecule, comprehensive AIM, NBO, NICS, GIMIC, and WBI calculations were conducted. Results for molecule **4c**, sharing similarities with its experimentally reported boron analogue,⁴⁴ are presented here; additional data for remaining molecules is available in the Electronic Supporting Information (ESI). Primarily, the Frontier Molecular Orbital (FMO) analysis in Figure-2 for **4c** reveals the HOMO, composed of π orbitals, entirely localized over the 4-membered ring (4-MR), while the LUMO composed of π^* orbitals localized over the Al and Ph ligands, yielding a HOMO-LUMO gap of 2.57 eV. Further insight into the HOMO composition is garnered through orbital composition analysis on Natural Atomic Orbitals (NAO) depicted in Figure S8. This analysis

indicates that 80.2% of the HOMO is attributed to the Si₂Al₂ ring, with each Si and Al contributing 18.9% and 21.2% individually. P_z orbitals of Si and Al exhibit the highest contributions across all cases. In comparison, Roesky's boron analogue³⁷ showcases a HOMO with a 66.8% contribution from an aromatic Si₂B₂ ring, featuring individual B and Si contributions of 20.3% and 12.8%. Similarly, Cui's molecule³⁰ reveals a HOMO with a 64.4% contribution from an aromatic Si₄ ring, with each Si contributing 11.9% and 20.3%.

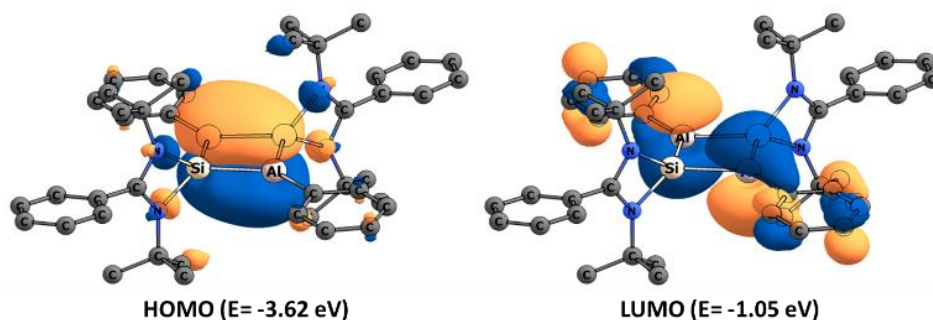


Figure 2. The HOMO and LUMO representation of molecule **4c** is shown here. The contour value of isosurface is 0.03. All the H-atoms are omitted for the purpose of clarity.

The WBI indices and Mayer bond order (MBI) for each Si-Al bond stand at 1.05 and 1.07, respectively, indicating a robust and unusually strong single Si-Al bond. To elucidate electron localization and delocalization (σ/π) in **4c**, we conducted Electron Localization Function (ELF) distribution analysis. Notably, along the Si-Al bond, a significant ELF value (depicted in red in Figure 3a) suggests a substantial covalent character, while Si-Si and Al-Al bonds exhibit negligible values, indicated by the absence of red color between these atoms. Furthermore, the 2.41e occupancy at each Si-Al bond, derived from the disynaptic basins calculation in the ELF analysis of **4c** (Figure 3b and S9), strongly indicates π -delocalization.

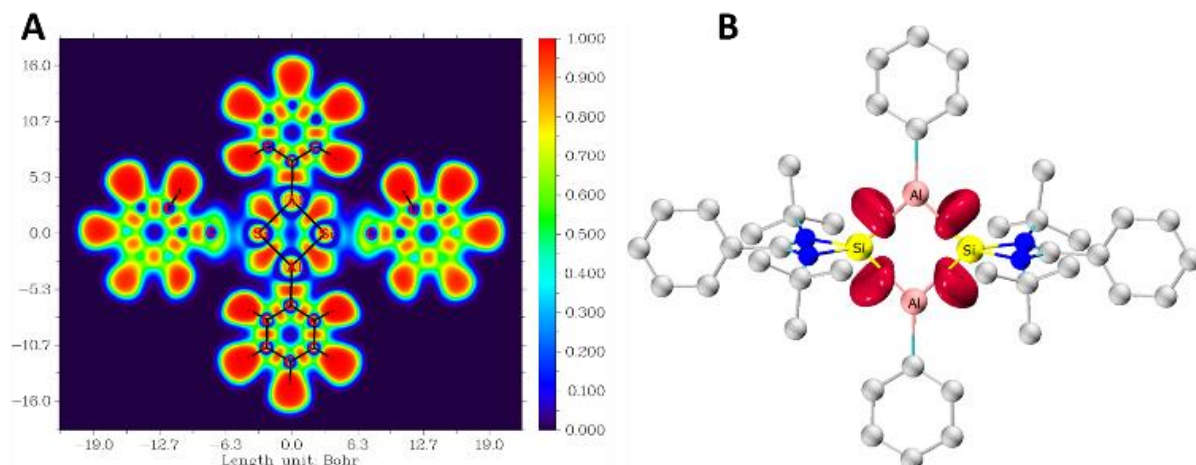


Figure 3. (a) ELF color-filled map of **4c**: red and blue indicate strong and weak electron localization, respectively. (b) ELF basin plot between Si-Al bonds with isosurface value 0.8.

The aromaticity of **4c** was assessed using Nucleus-Independent Chemical Shift (NICS) analysis. At the Si_2Al_2 ring center, NICS(0) and NICS(1) values are -12.7 and -9.9 ppm, respectively, while for the parent $\text{Si}_2\text{Al}_2\text{H}_4$, they are -14.2 and -16.4 ppm. This deviation signifies the substantial influence of the bulky Si-center group, perpendicular to the Si_2Al_2 ring, on NICS values, causing σ frame contamination, specifically 1 Å above or below the ring's center. Furthermore, considering the cautionary note from Stanger⁴⁶ regarding potential misinterpretation in single-point calculations of NICS at 0 or 1 Å, we opted for NICS-SCAN, providing a more comprehensive understanding. A 1D NICS scanning was performed from 0 to 6 Å above and below the center of the ring at intervals of 0.1 Å for better insight (refer to Figure 4 & S10). Furthermore, to facilitate a direct comparison between **4c** and the experimentally reported boron analogue,⁴⁴ we performed NICS calculations at the M06/def2TZVPP level of theory. The NICS(0) value for **4c** is -13.3, contrasting sharply with the -6.6 ppm value for the boron analogue, underscoring the substantial aromatic character in the **4c** molecule. The NICS values for **4c** across different theoretical levels are detailed in Table S3, demonstrating NICS(0) in the range of -12.3 to -13.3 ppm and NICS(1) in the range of -9.2 to -10.0 ppm. This suggests the basis set independence of the calculated NICS values in this case, reaffirming the 2π aromatic nature of the ring in all cases.

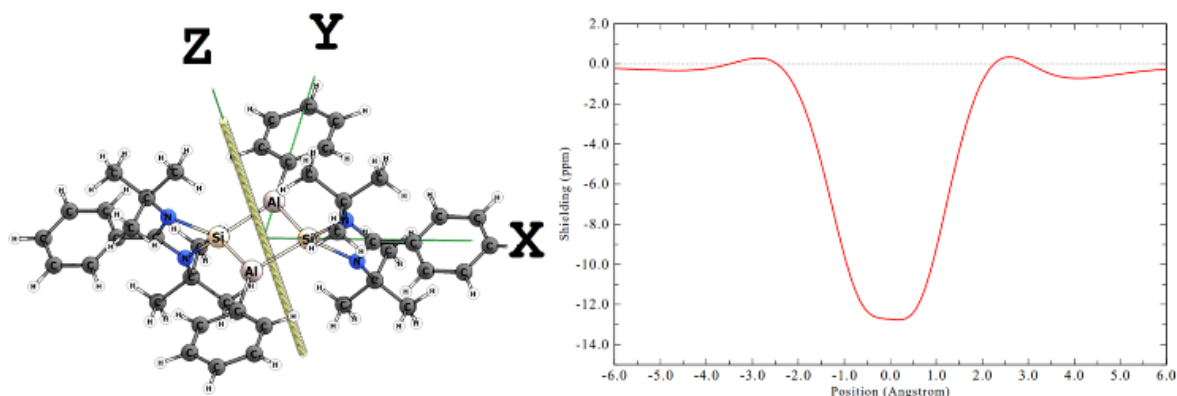


Figure 4. The NICS-SCAN profile for **4c** is shown here.

The streamline plot (Figure 5A) depicting the direction of current density was created through the GIMIC program. Notably, the Si_2Al_2 ring exhibits the maximum current flow. Furthermore, the ACID plot in Figure 5B showcases a clockwise direction of the induced current, robustly substantiating the aromaticity of this ring.

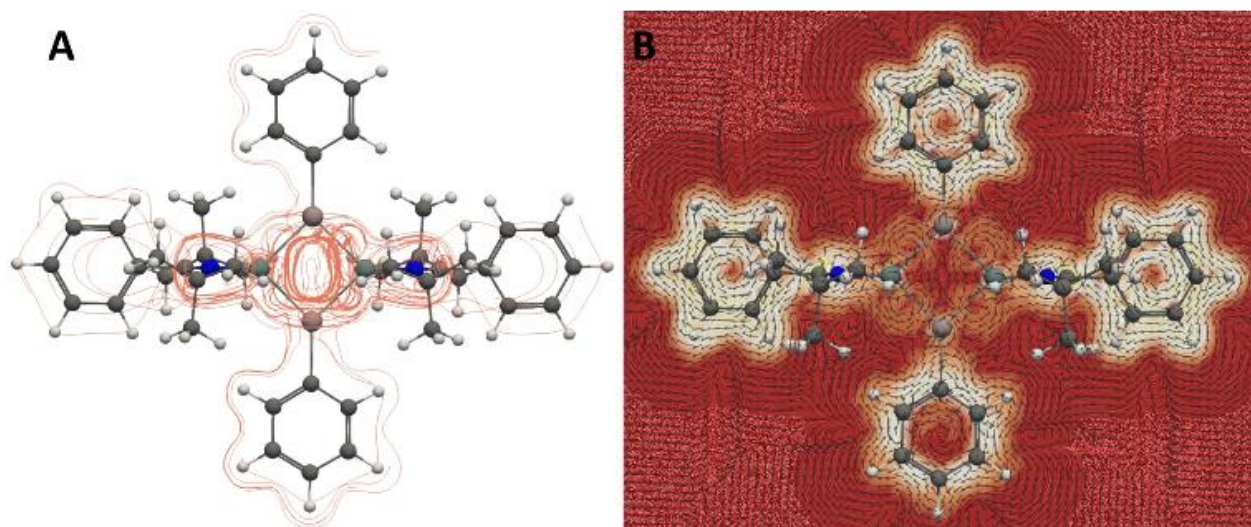


Figure 5. (A) The streamline plot of current density; (B) The ACID plot of **4c**.

The NBO calculations were employed to unravel the chemical bonding in **4c**. The second-order perturbation analysis unveils significant interactions. Specifically, the LP orbital, composed of the

pure P_z orbital of Si with an occupancy of 0.66e, engages with the LP^* orbitals, made from the pure P_z orbital of Al with an occupancy of 0.5e, resulting in a robust interaction energy of 142.6 kcal/mol. (refer to Table S5 in ESI) Additionally, the LP orbitals of both nitrogen atoms in the amidinated ligand interact with the LP^* orbital of Si, contributing interaction energies of 136.7 and 147.1 kcal/mol, thereby enhancing the overall stability of the system.

In summary, we have introduced a sophisticated molecular design strategy rooted in first principles, independent of experimental constraints. This four-stage framework, starting with the AINR method for formulating molecular structure, represents an original and new approach for the discovery of interesting compounds. Rigorous DFT calculations validate stability, ensuring reliability. The optimal molecule is refined iteratively, considering ligand tuning and energy and magnetic based criteria. Finally, practical applications are systematically identified based on structural attributes, reactivity and stability. This method, prioritizing efficiency, precision, and independence from experimental constraints, marks a significant stride toward more robust and accelerated molecular design processes.

Supporting Information.

The supporting information containing additional data and optimized Cartesian coordinates is available free of charge at [DOI].

AUTHOR INFORMATION

Corresponding Authors

*Kumar Vanka- Physical & Materials Chemistry Division, CSIR-National Chemical Laboratory, Dr. Homi Bhabha Road, Pashan, Pune, Maharashtra 411008, India; Academy of Scientific and Innovative Research (AcSIR). Sector 19, Kamla Nehru Nagar, Ghaziabad, Uttar Pradesh 201002, India;
ORCID: <https://orcid.org/0000-0001-7301-7573>;
Email: k.vanka@ncl.res.in

Author Contributions

The manuscript was written through contributions of all authors. All authors have given approval to the final version of the manuscript.

Notes

The authors declare no competing financial interest.

ACKNOWLEDGMENTS

K.V. is grateful to DST-SERB (CRG/2021/003255) and the CSIR-FIRST scheme for providing financial assistance. The support and the resources provided by the 'PARAM Brahma Facility' under the National Supercomputing Mission, Government of India at IISER Pune, are gratefully acknowledged. HS thanks UGC for SRF fellowship.

REFERENCES

- (1) Ess, D.; Gagliardi, L.; Hammes-Schiffer, S. Introduction: Computational Design of Catalysts from Molecules to Materials. *Chem. Rev.* **2019**, *119* (11), 6507–6508. <https://doi.org/10.1021/acs.chemrev.9b00296>.
- (2) Janet, J. P.; Chan, L.; Kulik, H. J. Accelerating Chemical Discovery with Machine Learning: Simulated Evolution of Spin Crossover Complexes with an Artificial Neural Network. *J. Phys. Chem. Lett.* **2018**, *9* (5), 1064–1071. <https://doi.org/10.1021/acs.jpcllett.8b00170>.
- (3) Ahn, S.; Hong, M.; Sundararajan, M.; Ess, D. H.; Baik, M. H. Design and Optimization of Catalysts Based on Mechanistic Insights Derived from Quantum Chemical Reaction Modeling. *Chem. Rev.* **2019**, *119* (11), 6509–6560. <https://doi.org/10.1021/acs.chemrev.9b00073>.
- (4) Durand, D. J.; Fey, N. Computational Ligand Descriptors for Catalyst Design. *Chem. Rev.* **2019**, *119* (11), 6561–6594. <https://doi.org/10.1021/acs.chemrev.8b00588>.
- (5) Freeze, J. G.; Kelly, H. R.; Batista, V. S. Search for Catalysts by Inverse Design: Artificial Intelligence, Mountain Climbers, and Alchemists. *Chem. Rev.* **2019**, *119* (11), 6595–6612. <https://doi.org/10.1021/acs.chemrev.8b00759>.
- (6) Wang, L. P.; Titov, A.; McGibbon, R.; Liu, F.; Pande, V. S.; Martínez, T. J. Discovering Chemistry with an Ab Initio Nanoreactor. *Nat. Chem.* **2014**, *6* (12), 1044–1048. <https://doi.org/10.1038/nchem.2099>.
- (7) Hohenberg, P.; W. Kohn. Inhomogeneous Electron Gas. *Phys. Rev.* **1964**, *136*, B864–B871.
- (8) W. Kohn AND L. J. Sham. Self-Consistent Equations Including Exchange and Correlation Effects. *Phys. Rev.* **1965**, *140*, A1133–A1138.
- (9) Schleyer, P. von R. Introduction : Aromaticity. *Chem. Rev.* **2001**, *101* (5), 1115–1118. <https://doi.org/10.1021/cr0103221>.
- (10) Bader, R. F. W. A Quantum Theory of Molecular Structure and Its Applications. *Chem. Rev.* **1991**, *91* (5), 893–928. <https://doi.org/10.1021/cr00005a013>.
- (11) Geerlings, P.; De Proft, F.; Langenaeker, W. Conceptual Density Functional Theory. *Chem. Rev.* **2003**, *103* (5), 1793–1873. <https://doi.org/10.1021/cr990029p>.
- (12) Faraday, M. XXVI. On New Compounds of Carbon and Hydrogen, and on Certain Other Products Obtained during the Decomposition of Oil by Heat . *Philos. Mag.* **1825**, *66* (329), 180–197. <https://doi.org/10.1080/14786442508673946>.
- (13) Heilbronner, E. % S Being the Standard Resonance Integral for a Pair Parallel. *Tetrahedron Lett.* **1964**, *29* (29), 1923–1928.
- (14) Hirsch, A.; Chen, Z.; Jiao, H. Spherical Aromaticity of Inorganic Cage Molecules. *Angew. Chemie - Int. Ed.* **2001**, *40* (15), 2834–2838. [https://doi.org/10.1002/1521-3773\(20010803\)40:15<2834::AID-ANIE2834>3.0.CO;2-H](https://doi.org/10.1002/1521-3773(20010803)40:15<2834::AID-ANIE2834>3.0.CO;2-H).
- (15) Ni, Y.; Gopalakrishna, T. Y.; Phan, H.; Kim, T.; Herng, T. S.; Han, Y.; Tao, T.; Ding, J.;

- Kim, D.; Wu, J. 3D Global Aromaticity in a Fully Conjugated Diradicaloid Cage at Different Oxidation States. *Nat. Chem.* **2020**, *12* (3), 242–248. <https://doi.org/10.1038/s41557-019-0399-2>.
- (16) Baird, N. C. Quantum Organic Photochemistry. II. Resonance and Aromaticity in the Lowest $3\pi\pi^*$ State of Cyclic Hydrocarbons. *J. Am. Chem. Soc.* **1972**, *94* (14), 4941–4948. <https://doi.org/10.1021/ja00769a025>.
- (17) Fowler, P. W.; Rees, C. W.; Soncini, A. Aromaticity of Organic Heterocyclothiazenes and Analogues. *J. Am. Chem. Soc.* **2004**, *126* (36), 11202–11212. <https://doi.org/10.1021/ja046399z>.
- (18) Zhang, Y.; Yu, C.; Huang, Z.; Zhang, W. X.; Ye, S.; Wei, J.; Xi, Z. Metalla-Aromatics: Planar, Nonplanar, and Spiro. *Acc. Chem. Res.* **2021**, *54* (9), 2323–2333. <https://doi.org/10.1021/acs.accounts.1c00146>.
- (19) Abersfelder, K.; White, A. J. P.; Rzepa, H. S.; Scheschkewitz, D. A Tricyclic Aromatic Isomer of Hexasilabenzene. *Science* (80-.). **2010**, *327* (5965), 564–566. <https://doi.org/10.1126/science.1181771>.
- (20) Zubarev, D. Y.; Averkiev, B. B.; Zhai, H. J.; Wang, L. S.; Boldyrev, A. I. Aromaticity and Antiaromaticity in Transition-Metal Systems. *Phys. Chem. Chem. Phys.* **2008**, *10* (2), 257–267. <https://doi.org/10.1039/b713646c>.
- (21) Roark, D. N.; Peddle, G. J. D. Reactions of 7,8-Disilabicyclo[2.2.2]Octa-2,5-Dienes. Evidence for the Transient Existence of a Disilene. *J. Am. Chem. Soc.* **1972**, *94* (16), 5837–5841. <https://doi.org/10.1021/ja00771a049>.
- (22) Schäfer, A.; Weidenbruch, M.; Peters, K.; von Schnering, H. -G. Hexa-tert-butylcyclotrisilane, a Strained Molecule with Unusually Long Si–Si and Si–C Bonds. *Angew. Chemie Int. Ed. English* **1984**, *23* (4), 302–303. <https://doi.org/10.1002/anie.198403021>.
- (23) Kira, M.; Iwamoto, T.; Kabuto, C. The First Stable Cyclic Disilene: Hexakis(Trialkylsilyl)Tetrasilacyclobutene. *J. Am. Chem. Soc.* **1996**, *118* (42), 10303–10304. <https://doi.org/10.1021/ja961913p>.
- (24) Wiberg, N.; Schuster, H.; Simon, A.; Peters, K. Hexa-tert-butylidisilane—the Molecule with the Longest Si–Si Bond. *Angew. Chemie Int. Ed. English* **1986**, *25* (1), 79–80. <https://doi.org/10.1002/anie.198600791>.
- (25) Yildiz, C. B.; Leszczyńska, K. I.; González-Gallardo, S.; Zimmer, M.; Azizoglu, A.; Biskup, T.; Kay, C. W. M.; Huch, V.; Rzepa, H. S.; Scheschkewitz, D. Equilibrium Formation of Stable All-Silicon Versions of 1,3-Cyclobutanediyl. *Angew. Chemie - Int. Ed.* **2020**, *59* (35), 15087–15092. <https://doi.org/10.1002/anie.202006283>.
- (26) Nukazawa, T.; Iwamoto, T. An Isolable Tetrasilicon Analogue of a Planar Bicyclo[1.1.0]Butane with π -Type Single-Bonding Character. *J. Am. Chem. Soc.* **2020**, *142* (22), 9920–9924. <https://doi.org/10.1021/jacs.0c03874>.
- (27) Kyushin, S.; Kurosaki, Y.; Otsuka, K.; Imai, H.; Ishida, S.; Kyomen, T.; Hanaya, M.; Matsumoto, H. Silicon–Silicon π Single Bond. *Nat. Commun.* **2020**, *11* (1). <https://doi.org/10.1038/s41467-020-17815-z>.
- (28) Zhang, Y.; Pannell, K. H. Formation of 1,2,4-Trisilacyclopentanes by Photolysis of $\text{FpCH}_2\text{SiR}_2\text{SiR}_2\text{SiR}_2\text{CH}_2\text{Fp}$ ($\text{Fp} = (\text{H}_5\text{-C}_5\text{H}_5)\text{Fe}(\text{CO})_2$). *Organometallics* **2002**, *21* (3), 503–510. <https://doi.org/10.1021/om0109657>.
- (29) Takeuchi, K.; Ichinohe, M.; Sekiguchi, A. Access to a Stable Si_2N_2 Four-Membered Ring with Non-Kekulé Singlet Biradical Character from a Disilyne. *J. Am. Chem. Soc.* **2011**,

- 133 (32), 12478–12481. <https://doi.org/10.1021/ja2059846>.
- (30) Hinz, A.; Kuzora, R.; Rölke, A. K.; Schulz, A.; Villinger, A.; Wustrack, R. Synthesis of a Silylated Phosphorus Biradicaloid and Its Utilization in the Activation of Small Molecules. *Eur. J. Inorg. Chem.* **2016**, *2016* (22), 3611–3619. <https://doi.org/10.1002/ejic.201600321>.
- (31) Olah, G. A.; Staral, J. S. Novel Aromatic Systems. 4. Cyclobutadiene Dications. *J. Am. Chem. Soc.* **1976**, *98* (20), 6290–6304. <https://doi.org/10.1021/ja00436a037>.
- (32) George A. Olah, G. D. M. Stable Carbonium Ions. CI. Tetraphenylcyclobutadiene Dication. *J. Am. Chem. Soc.* **1970**, *92* (5), 1430–1432. <https://doi.org/10.1021/ja00708a070>.
- (33) Li, Y.; Dong, S.; Guo, J.; Ding, Y.; Zhang, J.; Zhu, J.; Cui, C. π -Aromaticity Dominating in a Saturated Ring: Neutral Aromatic Silicon Analogues of Cyclobutane-1,3-Diyls. *J. Am. Chem. Soc.* **2023**, *145* (39), 21159–21164. <https://doi.org/10.1021/jacs.3c06555>.
- (34) Zhang, S. H.; Xi, H. W.; Lim, K. H.; So, C. W. An Extensive n , π , σ -Electron Delocalized Si₄ Ring. *Angew. Chemie - Int. Ed.* **2013**, *52* (47), 12364–12367. <https://doi.org/10.1002/anie.201305567>.
- (35) Hess, B. A.; Ewig, C. S.; Schaad, L. J. An Ab Initio Study of the Cyclobutadiene Dianion and Dication. *J. Org. Chem.* **1985**, *50* (26), 5869–5871. <https://doi.org/10.1021/jo00350a087>.
- (36) Dabringhaus, P.; Zedlitz, S.; Giarrana, L.; Scheschkewitz, D.; Krossing, I. Low-Valent MxAl₃ Cluster Salts with Tetrahedral [SiAl₃]⁺ and Trigonal-Bipyramidal [M₂Al₃]₂⁺ Cores (M=Si/Ge). *Angew. Chemie - Int. Ed.* **2023**, *62* (8). <https://doi.org/10.1002/anie.202215170>.
- (37) Li, J.; Zhong, M.; Keil, H.; Zhu, H.; Herbst-Irmer, R.; Stalke, D.; De, S.; Koley, D.; Roesky, H. W. (PhC(N: T Bu)2Al)2(SiH2)4 Six-Membered Heterocycle: Comparable in Structure to Cyclohexane. *Chem. Commun.* **2019**, *55* (16), 2360–2363. <https://doi.org/10.1039/c8cc10124h>.
- (38) Chu, T.; Korobkov, I.; Nikonov, G. I. Oxidative Addition of σ Bonds to an Al(I) Center. *J. Am. Chem. Soc.* **2014**, *136* (25), 9195–9202. <https://doi.org/10.1021/ja5038337>.
- (39) Xiong, Y.; Yao, S.; Driess, M. Versatile Conversion of N-Heterocyclic Silylene to Silyl Metal Compounds by Insertion of Divalent Silicon into Metal-Carbon and Metal-Hydrogen Bonds. *Chem. - A Eur. J.* **2012**, *18* (11), 3316–3320. <https://doi.org/10.1002/chem.201103656>.
- (40) Zeng, X.; Kieffer, R.; Glettner, B.; Nürnberger, C.; Liu, F.; Pelz, K.; Prehm, M.; Baumeister, U.; Hahn, H.; Lang, H.; Gehring, G. A.; Weber, C. H. M.; Hobbs, J. K.; Tschierske, C.; Ungar, G. Complex Multicolor Tilings and Critical Phenomena in Tetraphilic Liquid Crystals. *Science* (80-.). **2011**, *331* (6022), 1302–1306. <https://doi.org/10.1126/science.1193052>.
- (41) Keuter, J.; Schwedtmann, K.; Hepp, A.; Bergander, K.; Janka, O.; Doerenkamp, C.; Eckert, H.; Mück-Lichtenfeld, C.; Lips, F. Diradicaloid or Zwitterionic Character: The Non-Tetrahedral Unsaturated Compound [Si₄{N(SiMe₃)Dipp}₄] with a Butterfly-Type Si₄ Substructure. *Angew. Chemie - Int. Ed.* **2017**, *56* (44), 13866–13871. <https://doi.org/10.1002/anie.201705787>.
- (42) Keuter, J.; Hepp, A.; Daniliuc, C. G.; Feldt, M.; Lips, F. Cycloadditions with a Stable Charge-Separated Cyclobutadiene-Type Amido-Substituted Silicon Ring Compound. *Angew. Chemie - Int. Ed.* **2021**, *60* (40), 21761–21766.

- <https://doi.org/10.1002/anie.202104341>.
- (43) Hückel, E. Quantentheoretische Beiträge Zum Benzolproblem - I. Die Elektronenkonfiguration Des Benzols Und Verwandter Verbindungen. *Zeitschrift für Phys.* **1931**, *70* (3–4), 204–286. <https://doi.org/10.1007/BF01339530>.
- (44) Kushvaha, S. K.; Kallenbach, P.; Rohman, S. S.; Pandey, M. K.; Hendi, Z.; Rüttger, F.; Herbst-Irmer, R.; Stalke, D.; Parameswaran, P.; Roesky, H. W. A Neutral Planar Four-Membered Si₂B₂ 2 π -Aromatic Ring. *J. Am. Chem. Soc.* **2023**, *145* (47), 25523–25527. <https://doi.org/10.1021/jacs.3c09131>.
- (45) Fan, J.; Yue, L.; Liu, C.; Rao, B.; Zhou, G.; Li, A.; Su, B. Isolation of Fluorescent 2 π -Aromatic 1,3-Disiladiboretenes. *J. Am. Chem. Soc.* **2023**, 6–11. <https://doi.org/10.1021/jacs.3c09747>.
- (46) Stanger, A. Nucleus-Independent Chemical Shifts (NICS): Distance Dependence and Revised Criteria for Aromaticity and Antiaromaticity. *J. Org. Chem.* **2006**, *71* (3), 883–893. <https://doi.org/10.1021/jo051746o>.